Toward a Stochastic Parameterization for Oceanic Deep Convection

Quentin Jamet, Etienne Mémin, Franck Dumas, Long Li, and Pierre Garreau

Abstract Current climate models are known to systematically overestimate the rate of deep water formation at high latitudes in response to too deep and too frequent deep convection events. We propose in this study to investigate a misrepresentation of deep convection in Hydrostatic Primitive Equation (HPE) ocean and climate models due to the lack of constraints on vertical dynamics. We discuss the potential of the Location Uncertainty (LU) stochastic representation of geophysical flow dynamics to help in the process of re-introducing some degree of non-hydrostatic physics in HPE models through a pressure correction method. We then test our ideas with idealized Large Eddy Simulations (LES) of buoyancy driven free convection with the CROCO modeling platform. Preliminary results at LES resolution exhibit a solution obtained with our Quasi-nonhydrostatic (Q-NH) model that tends toward the reference non-hydrostatic (NH) model. As compared to a pure hydrostatic setting, our Q-NH solution exhibits vertical convective plumes with larger horizontal structure, a better spatial organization and a reduced intensity of their associated vertical velocities. The simulated Mixed Layer Depth (MLD) deepening rate is however too slow in our Q-NH experiment as compared to the reference NH, a behaviour that opposes to that of hydrostatic experiments of producing too fast MLD deepening rate. These preliminary results are encouraging, and support future efforts in the direction of enriching coarse resolution, hydrostatic ocean and climate models with a stochastic representation of non-hydrostatic physics.

Q. Jamet (✉)
INRIA, ODYSSEY Group, Plouzané, France
e-mail: quentin.jamet@inria.fr

E. Mémin · L. Li
INRIA, ODYSSEY Group, Rennes, France

F. Dumas
SHOM, Brest, France

P. Garreau
Laboratoire d'Océanographie Physique et Spatiale, IFREMER, Plouzané, France

B. Chapron et al. (eds.), *Stochastic Transport in Upper Ocean Dynamics II*,
Mathematics of Planet Earth 11, https://doi.org/10.1007/978-3-031-40094-0_6

1 Introduction

Deep ocean convection is a crucial mechanism for large scale ocean circulation and climate. It controls the rate of deep ocean water masses formation, sequestrating atmospheric properties such as heat and carbon in the abyssal ocean. In the North Atlantic basin, deep ocean convection in the Labrador Sea and the Nordic Seas is part of the large scale Atlantic Meridional Overturning Circulation (AMOC), an oceanic metric with many climate implications (Zhang et al. 2019). Coarse resolution (i.e. $\Delta x \sim \mathcal{O}(100)$ km) climate models are known to overestimate the rate of deep water formation at high latitudes in response to too deep and too frequent convective events (Heuzé 2017; 2021), a bias that is expected to worsen with next generation climate models with ocean components at higher resolution (Masson-Delmotte et al. 2021). Among other possibilities (e.g. preconditioning, air-sea interactions), we explore in this paper the possible misrepresentation of deep ocean convection in current climate models in response to their hydrostatic formulation.

Ocean modulus of current climate models solve the Hydrostatic Primitive Equations (HPE), a simplified version of the full Navier-Stokes equations (NS). Geophysical fluids have specific characteristics that allow some approximations from the general NS, leading to drastic simplifications in their numerical implementation which, in turn, allow us to model the global ocean at climate scales (i.e. for several decades/centuries) with the currently available computational resources. Among those approximations is the hydrostatic balance which arises from the relatively thin thickness of the ocean ($\mathcal{H} \sim \mathcal{O}(1)$ km) as compared to the horizontal extension of its large scale dynamics ($\mathcal{L} \sim \mathcal{O}(1000)$ km for gyres and $\mathcal{L} \sim \mathcal{O}(10-100)$ km for ocean mesoscale eddies). The aspect ratio $\delta = \frac{\mathcal{H}}{\mathcal{L}}$ is thus orders of magnitude smaller than unity. Scaling the vertical velocity $W = \delta U$, with U the typical horizontal velocity of the flow, leads to small contribution of vertical acceleration as compared to horizontal components. For a regime satisfying such a scaling, only vertical pressure gradients are able to balance gravitational acceleration in the vertical component of the NS equations, and the system can be simplified as:

$$\partial_t u + \boldsymbol{\nabla} \cdot (\boldsymbol{u} u) - f v = -\frac{1}{\rho_0} \partial_x p + \mathcal{F}_u + \mathcal{D}_u, \tag{1a}$$

$$\partial_t v + \boldsymbol{\nabla} \cdot (\boldsymbol{u} v) + f u = -\frac{1}{\rho_0} \partial_y p + \mathcal{F}_v + \mathcal{D}_v, \tag{1b}$$

$$0 = -\frac{1}{\rho_0} \partial_z p - b, \tag{1c}$$

where $\boldsymbol{u} = (u, v, w)$ is the three-dimensional velocity field, $f = 2\Omega sin(\theta)$ is the traditional Coriolis pseudo-force, p is pressure, $b = \frac{\rho - \rho_0}{\rho_0} g$ is the *buoyancy* defined for Boussinesq fluids (i.e. when density ρ is replaced by its constant value ρ_0,

unless multiplied by gravity in which case it is expressed as density anomaly $\frac{\rho-\rho_0}{\rho_0}$), and $\mathcal{F}$ and $\mathcal{D}$ are forcing and dissipative processes, respectively. Equations (1a)–(1c) are the HPE momentum equations used in current climate models. From a numerical viewpoint, using HPE instead of general NS or other Non-Hydrostatic (NH) sets of equation greatly simplifies the procedure as only (1a) and (1b) have to be stepped forward in time for each discretized ocean layers, while (1c) is used (diagnostically) to obtain the pressure field through vertical integration of density variations subject to gravitational acceleration. In HPE models, convection is part of the parameterized (i.e. unresolved) three-dimensional turbulence and mixing processes which are encapsulated in $\mathcal{D}_{u,v}$. Usually, these operators are formulated with a down-gradient approach, where the vertical fluxes of a scalar θ are parameterized as $\overline{w'\theta'} = -K_\theta \partial_z \overline{\theta}$, with $\overline{\theta}$ the local, resolved field. Several models can be used to estimate the dissipation coefficient K_θ (e.g. TKE (Gaspar et al. 1990), GLS (Umlauf and Burchard 2003), KPP (Large et al. 1994)), but in case of convection, this coefficient is usually set to an unrealistically large value (0.1 to 10 $\mathrm{m^2 s^{-1}}$) to quickly restore static instabilities associated with convective processes and avoid model instabilities. More recently, Giordani et al. (2020) proposed an oceanic application of the eddy-diffusivity mass-flux formulation initially derived by the atmospheric community (e.g., Hourdin et al. 2006, Suselj et al. 2019), which allows a better representation of vertical advective fluxes associated with convection. The approximations leading to HPE are likely to be satisfied in most of the ocean where vertical velocities are small and their spatial patterns are of small scales. However, for the case of deep ocean convection where vertical velocities can reach $W \sim \mathcal{O}(10\ \mathrm{cm\ s^{-1}})$ and over horizontal scales of $\mathcal{L} \sim \mathcal{O}(1\ \mathrm{km})$, such approximations become questionable. In case such approximations turn out to be violated, it becomes necessary to find ways of re-introducing some form of non-hydrostasy within HPE.

Klingbeil and Burchard (2013) have proposed a direct implementation of full non-hydrostatic effects into an HPE model through a pressure correction method. Instead of solving the full three-dimentional velocity field equations

$$\partial_t u + \boldsymbol{\nabla} \cdot (\boldsymbol{u} u) - f v + \tilde{f} w = -\frac{1}{\rho_0} \partial_x p + \mathcal{F}_u + \mathcal{D}_u, \tag{2a}$$

$$\partial_t v + \boldsymbol{\nabla} \cdot (\boldsymbol{u} v) + f u \qquad = -\frac{1}{\rho_0} \partial_y p + \mathcal{F}_v + \mathcal{D}_v, \tag{2b}$$

$$\partial_t w + \underline{\boldsymbol{\nabla} \cdot (\boldsymbol{u} w)} \qquad - \tilde{f} u = -\frac{1}{\rho_0} \partial_z p - b + \mathcal{F}_w + \underline{\mathcal{D}_w}, \tag{2c}$$

where $\tilde{f} = 2\Omega cos(\theta)$ is the non-traditional Coriolis pseudo-force (shown for consistency but not considered in the following), and non-hydrostatic contributions are shown in blue. To avoid the complexity of solving a three dimensional Poisson equation to recover the non-hydrostatic pressure (as usually done in NH pressure correction methods, e.g. Marshall et al. 1997) Klingbeil and Burchard (2013)

proposed to account for non-hydrostatic pressure correction through a vertical integration of a so-called *non-hydrostatic buoyancy*, i.e. following the strategy of HPE models. This strategy offers a general implementation of NH physics in HPE, but still suffers from numerical instabilities in the case of strongly non-hydrostatic dynamics. For the case of deep ocean convection, it can be shown that further simplifications can be made by only accounting for the horizontal viscosity acting on the vertical velocities in the computation of the NH pressure correction (through vertical integration ; Pierre Garreau, personal communication). As will be shown later through the analysis of different idealized Large Eddy Simulations (LES), HPE models tend to produce convective plumes near the grid size of the model, leading to unstructured (on the horizontal) convective cells. From one grid point to the next, vertical velocities could be of opposite sign leading to intense horizontal gradients. Including a horizontal viscous operator on the HPE vertical velocities (we recall here that in HPE vertical velocities are diagnosed from the horizontal velocity field though continuity) leads to a broadening of the convective plumes and a more realistic horizontal organization. In other words, when convective plumes start to form, they '*entrain*' the neighboring points thus communicating horizontally their vertical momentum. Such a process can be seen as a simplified entrainment/detrainment mechanism discussed by Giordani et al. (2020) for the case of edddy-diffusivity mass-flux parameterization. In the present study, we consider the approach of Klingbeil and Burchard (2013) as a starting point and discuss a strategy to extend this idea in the context of a stochastic parameterization. The results presented here are all obtained at LES resolution, such that a clear connection with climate scale regimes is still lacking. However, these results provide a first step toward the development of robust stochastic parameterization for climate models, which will be the subject of dedicated studies.

The paper is organized as follow. In Sect. 2 we briefly recall the Location Uncertainty (LU; Mémin 2014, Bauer et al. 2020, Resseguier et al. 2017) framework used to represent the inertial and dissipative effects on vertical momentum (underlined terms in (2c)) as a result of a strong noise regime or for application to flow dynamics where the hydrostatic approximation becomes questionable. Section 3 is dedicated to the numerical implementation of the stochastic, non-hydrostatic pressure correction into the terrain-following Coastal and Regional Ocean Community (CROCO), along with the description of the simulations we have conducted. Preliminary results are described and discussed in Sect. 4. We summarize our paper and provide some perspectives for further work in Sect. 5.

2 Stochastic Formulation of Direct Non-hydrostatic Pressure Correction

Following Mémin (2014), the stochastic version of the horizontal momentum equation (in vector notation) reads:

$$\mathbb{D}_t \boldsymbol{u}_h + f\boldsymbol{k} \times (\boldsymbol{u}_h \mathrm{d}t + \boldsymbol{\sigma} \mathrm{d}\boldsymbol{B}_t^H) = -\frac{1}{\rho_0} \boldsymbol{\nabla}_H (p \mathrm{d}t + \mathrm{d}p_t^\sigma), \tag{3}$$

with $\boldsymbol{u}_h = (u, v, 0)$, $\mathbb{D}_t$ the stochastic transport operator defined as:

$$\mathbb{D}_t \boldsymbol{u}_h = \mathrm{d}_t \boldsymbol{u}_h + (\boldsymbol{u}^\star \mathrm{d}t + \boldsymbol{\sigma} \mathrm{d}\boldsymbol{B}_t) \cdot \boldsymbol{\nabla} \boldsymbol{u}_h - \frac{1}{2} \boldsymbol{\nabla} \cdot (\boldsymbol{a} \boldsymbol{\nabla} \boldsymbol{u}_h) \mathrm{d}t, \tag{4}$$

with $\boldsymbol{u}^\star$ the incompressible (i.e. $\boldsymbol{\nabla} \cdot \boldsymbol{\sigma} \mathrm{d}\boldsymbol{B}_t = 0$) modified advection defined as:

$$\boldsymbol{u}^\star = \boldsymbol{u} - \frac{1}{2} \boldsymbol{\nabla} \cdot \boldsymbol{a} \tag{5}$$

where $\boldsymbol{u} = (\boldsymbol{u}_h, w)$ is the three dimensional velocity field, $\boldsymbol{\sigma} \mathrm{d}\boldsymbol{B}_t$ represents the stochastic flow and $\boldsymbol{a}$ its associated variance tensor. The term $\frac{1}{2} \boldsymbol{\nabla} \cdot \boldsymbol{a}$ can be interpreted as an equivalent of the Stokes drift for an inhomogeneous random fast component $\boldsymbol{\sigma} \mathrm{d}\boldsymbol{B}_t$ (Bauer et al. 2020).

The introduction of the stochastic pressure $\mathrm{d}p_t^\sigma$ in (3) requires some discussion. This stochastic pressure is associated with the small scale velocity component encoded through the noise. Following Resseguier et al. (2017), for smooth-in-time momentum equation subject to a classical deterministic large scale momentum equation, its (three dimensional) gradient can be expressed as:

$$-\frac{1}{\rho_0} \boldsymbol{\nabla} \mathrm{d}p_t^\sigma = (\boldsymbol{\sigma} \mathrm{d}\boldsymbol{B}_t) \cdot \boldsymbol{\nabla} \boldsymbol{u} + \mathbf{f} \times \boldsymbol{\sigma} \mathrm{d}\boldsymbol{B}_t \tag{6}$$

such that its interpretation (and scalling) should be related to the processes the stochastic formulation aims at representing. In the context of large scale modelling parameterization such as Tucciarone et al. (2023), the stochastic Primitive Equations they derived is meant to represent the effects of meso (and potentially submeso) scale eddies onto the large scale gyre circulation. The usual hydrostatic arguments are thus used, such that the vertical gradient of the stochastic pressure is identically zero (i.e. $\partial_z \mathrm{d}p_t^\sigma = 0$) and its horizontal gradient is strictly balanced by the stochastic Coriolis pseudo-force. Here, we are interested in relaxing the hydrostatic approximation on the noise structure, but retaining it for the smooth-in-time, resolved flow, and derive the stochastic equation for the vertical momentum. As a first step in this direction, we will not include the contribution of the non-traditional Coriolis pseudo-force. After some manipulations, we obtain the following equation for the vertical momentum:

$$(-\frac{1}{2} \boldsymbol{\nabla} \cdot \boldsymbol{a}) \cdot \boldsymbol{\nabla} w \mathrm{d}t - \frac{1}{2} \boldsymbol{\nabla} \cdot (\boldsymbol{a} \boldsymbol{\nabla} w) \mathrm{d}t + \underline{\boldsymbol{\sigma} \mathrm{d}\boldsymbol{B}_t \cdot \boldsymbol{\nabla} w} = (-\frac{1}{\rho_0} \partial_z p - b) \mathrm{d}t - \underline{\frac{1}{\rho_0} \partial_z \mathrm{d}p_t^\sigma}, \tag{7}$$

Black terms in (7) are associated with hydrostatic physics and terms in blue are the different stochastic contributions that emerge when applying non-hydrostatic

thinkings on the stochastic noise. The left-hand side terms corresponds to the vertical acceleration with a scaling such that the noise vertical acceleration is strong compared to the large-scale vertical acceleration terms. Note that the two underlined terms in (7) are Brownian terms emerging from the stochastic pressure formulation (6) on the right-hand side and from the vertical velocity transport by the noise on the left-hand side. The two other blue terms on the LHS are associated with modified advection and dissipation (projected on the vertical velocity w) that emerged through the three dimensional generalization of (4):

$$\mathbb{D}_t \boldsymbol{u} = \mathrm{d}_t \boldsymbol{u}_h + \boldsymbol{u} \cdot \nabla \boldsymbol{u}_h + (-\frac{1}{2}\nabla \cdot \boldsymbol{a}\mathrm{d}t + \boldsymbol{\sigma}\mathrm{d}\boldsymbol{B}_t) \cdot \nabla \boldsymbol{u} - \frac{1}{2}\nabla \cdot (\boldsymbol{a}\nabla \boldsymbol{u})\mathrm{d}t, \tag{8}$$

where the material derivative of vertical velocities associated with the resolved flow (i.e. $\mathrm{d}_t w + \boldsymbol{u} \cdot \nabla w$) has been neglected.

The noise being given (and calibrated from data or a known relation), from (7), it is thus possible to compute the various Brownian terms on the LHS, then to integrate vertically the results to obtain a 3D map of the modified pressure field as a result of the noise transport. Separating safely the martingale part (Brownian terms) from the smooth-in-time components ("dt" terms), we have

$$\mathrm{d}p_t^{\sigma}(z) = \mathrm{d}p_t^{\sigma}|_{z=\eta} + \rho_0 \int_z^{\eta} (\boldsymbol{\sigma}\mathrm{d}\boldsymbol{B}_t \cdot \nabla w)\, dz', \tag{9}$$

for the martingale component, and

$$p(z)dt = p|_{z=\eta}dt + \rho_0 g(\eta - z)dt + \rho_0 \int_z^{\eta} \left(bdt - \underbrace{\left((\frac{1}{2}\nabla \cdot \boldsymbol{a}) \cdot \nabla w \mathrm{d}t + \frac{1}{2}\nabla \cdot (\boldsymbol{a}\nabla w)\mathrm{d}t \right)}_{b_{NH}} \right) dz', \tag{10}$$

for the smooth-in-time component. The three last terms on the RHS of (10) can be compared to the deterministic non-hydrostatic pressure correction of Klingbeil and Burchard (2013), although the material derivative of w associated with resolved flow is not included in our stochastic formulation. It can be noted that our formulation involves a 3D diffusion of the vertical velocity ensuing from the noise action as well as the contribution of the modified Ito-Stokes term arising from the spatial inhomogeneity of the noise. Both (9) and (10) should be integrated with appropriate boundary conditions at η to incorporate fast and smooth-in-time surface pressure contributions (such as surface waves or atmospheric pressure loading, respectively), but such contributions can be neglected at first approximation without loss of generality. Results of (9) and (10) can then be used to feedback onto the horizontal momentum equation (3) solved by an hydrostatic model. Assuming a strict separation of the martingale part and the smooth-in-time component, only (10)

is assumed to feedback onto the resolved flow. The martingale components are assumed to balance each other, thus not affecting the resolved flow. This assumption can be interpreted as a Large Eddy Simulation (LES) -like approach, as discussed by Bauer et al. (2020).

As a preliminary step, we will further simplify the structure of the variance tensor $\boldsymbol{a}$ in order to reduce the second and third terms on the RHS of (10) to a simple Laplacian viscosity—induced here by the noise contribution. This simplification is motivated in the following. In the LU framework, the strength of the noise is measured by its (one-point co-) variance, such that

$$\boldsymbol{a}(\boldsymbol{x},t) \triangleq \breve{\boldsymbol{q}}(\boldsymbol{x},\boldsymbol{x},t), \tag{11}$$

with $\breve{\boldsymbol{q}}(\boldsymbol{x},\boldsymbol{x},t)$ a matrix kernel defined as

$$\breve{\boldsymbol{q}}(\boldsymbol{x},\boldsymbol{x},t) \triangleq \int_{\Omega} \breve{\boldsymbol{\sigma}}(\boldsymbol{x},\boldsymbol{x}',t)\breve{\boldsymbol{\sigma}}(\boldsymbol{x},\boldsymbol{x}',t)^T d\boldsymbol{x}', \tag{12}$$

with $\breve{\boldsymbol{\sigma}}(\cdot,\cdot,t)$ a bounded matrix kernel defining the correlation deterministic integral operator $\boldsymbol{\sigma}_t : L^2(\Omega) \rightarrow L^2(\Omega)$

$$\boldsymbol{\sigma}_t \boldsymbol{f}(\boldsymbol{x}) \triangleq \int_{\Omega} \breve{\boldsymbol{\sigma}}(\boldsymbol{x},\boldsymbol{y},t)\boldsymbol{f}(\boldsymbol{y})d\boldsymbol{y}, \quad \forall \boldsymbol{f} \in (L^2(\Omega)). \tag{13}$$

(See, e.g. Bauer et al. 2020, Mémin 2014, Resseguier et al. 2017, for further details). Although the previous definition of the noise is general, it is possible, through the Mercer's theorem, to express the noise variance as a spectral decomposition of the form:

$$\boldsymbol{a}(\boldsymbol{x},t) = \sum_{n\in\mathbb{N}} \lambda_n(t)\boldsymbol{\phi}_n(\boldsymbol{x},t)\boldsymbol{\phi}_n^T(\boldsymbol{x},t), \tag{14}$$

where $\boldsymbol{\phi}_n(\boldsymbol{x},t)$ define an orthonormal eigenfunction basis of the correlation operator, $\boldsymbol{\sigma}_t$, with $\lambda_n(t)$ their corresponding eigenvalues. For a stationary noise, this reduces to a classical POD (or EOF) decomposition, in which the eigenfunctions are the solution of the eigenvalue problem

$$\int_{\Omega} \boldsymbol{K}(\boldsymbol{x},\boldsymbol{x}')\boldsymbol{\phi}_n(\boldsymbol{x}')d\boldsymbol{x}' = \lambda_n\boldsymbol{\phi}_n(\boldsymbol{x}) \tag{15}$$

with $\boldsymbol{K}$ the two-point correlation tensor.

The next step is to assume isotropy and homogeneity of the noise structure, in which case the Fourier modes $\boldsymbol{\phi}_n = e^{2\pi i\boldsymbol{k}\cdot\boldsymbol{x}}$ are a natural choice to satisfy (15), which implies (Berkooz et al. 1993):

$$\boldsymbol{K} = \sum_n \lambda_n e^{2\pi i\boldsymbol{k}\cdot\boldsymbol{x}} e^{-2\pi i\boldsymbol{k}\cdot\boldsymbol{x}'}. \tag{16}$$

Under isotropic condition, the variance of the divergence-free noise is constant and diagonal, such that the first term associated with b_{NH} in (10) is identically zero, and the noise induced dissipation reduces to:

$$\frac{1}{2}\nabla \cdot (\boldsymbol{a}\nabla w) = \nu \Delta w, \tag{17}$$

with ν the isotropic, homogeneous noise induced momentum dissipation. Through vertical integration of (17), we recover part of the non-hydrostatic pressure correction proposed by Klingbeil and Burchard (2013), which in the present case mimic entrainement/detrainement of convective plumes leading to changes in their spatial organization. This modified HPE will be termed Quasi-Nonhydrostatic (Q-NH), by analogy with the Quasi-Hydrostatic (QH) of Marshall et al. (1997) where non-traditional Coriolis terms are added into the HPE.

3 Numerical Implementation and Simulations

Our objective is to implement this stochastic, non-hydrostatic pressure correction in the hydrostatic kernel of the Coastal and Regional Ocean Community model (CROCO ; http://www.croco-ocean.org). CROCO is a new ocean model that builds upon the structure of the ROMS-AGRIF primitive equation solver (Shchepetkin and McWilliams 2005, Debreu et al. 2012). The non-hydrostatic, non-Boussinesq (NQB ; Auclair et al. 2018) capabilities of CROCO will also be used to construct a reference simulation for validation (see Table 1). We review in the following some important steps for the implementation of the stochastic pressure correction within CROCO, discuss their implications and how we treat the pressure correction within the hydrostatic CROCO kernel.

3.1 Stochastic, Non-hydrostatic Pressure Correction

In its hydrostatic mode, CROCO computes $\frac{p}{\rho_0}$, from which horizontal gradients directly feed the baroclinic horizontal momentum equation (i.e. (2a) and (2b)). Our strategy is to include the NH pressure correction via a modified density/buoyancy field, such that the pressure field becomes:

$$\frac{p(z)}{\rho_0} = \frac{p|_{z=\eta}}{\rho_0} + \int_z^\eta \frac{(\rho - \rho_0) - b_{NH}}{\rho_0} g \, dz', \tag{18}$$

with b_{NH} collecting the different contributions of the vertical momentum equation (w_trends) contributing in the pressure correction, normalized by gravity:

$$b_{NH} = \frac{1}{g} \sum w\_trends, \tag{19}$$

where the horizontal dissipation of vertical velocity (e.g. Eq. (17)) is computed along sigma coordinates. Our strategy is similar to Delorme et al. (2021), who derived a Quasi-Hydrostatic version of CROCO by including the non-traditional Coriolis effects through buoyancy correction.

Let us note that b_{NH} is abusively denoted through a buoyancy variable, however it corresponds to corrections brought by the noise to the usual hydrostatic pressure. Such a correction should not be interpreted as an actual modification of the density/buoyancy field of the stratified ocean. Thus, the stochastic contribution is not included in the specific treatment of baroclinic-barotropic mode coupling of CROCO, which aims at accounting for the non-uniform density field for the propagation of gravity waves (Gill 1982), ultimately reducing the usual mode-coupling error associated with mode-splitting schemes (Shchepetkin and McWilliams 2005). In other words, we do not expect this '*non-hydrostatic buoyancy*' to affect gravity wave's propagation.

Finally, CROCO uses a third-order predictor-corrector (LF-AM3) time-stepping scheme for tracers and baroclinic momentum. This scheme consists of a Leapfrog (LF) predictor with 3rd-order Adams-Moulton (AM) interpolation. It also uses split-explicit techniques to robustly couple the slow, baroclinic and the fast, barotropic modes associated with the time evolving non-linear free surface. A complete description of the several stages of CROCO time-stepping can be found in Section 5 of Shchepetkin and McWilliams (2005). This predictor-corrector, split-explicit scheme implies some tendency terms of the baroclinic mode are computed twice to step forward baroclinic momentum and tracer equations from time step t to time step $t + \Delta t$. The first computation is performed at the *prediction* stage, and the second computation is performed at the *correction* stage. These tendencies include pressure gradients. To avoid double counting the stochastic pressure correction and for stability reasons, the modified non-hydrostatic buoyancy is computed only at the *correction* stage.

3.2 Numerical Experiments

The numerical experiments we used to test our stochastic non-hydrostatic pressure correction are oceanic deep convection events. The configuration is inspired by free convection studies (e.g. Souza et al. 2020) where an horizontally uniform surface cooling is applied to a constantly stratified, horizontally uniform ocean. Although our interest is on deep ocean convection rather than mixed layer free convection, we have adopted an horizontally uniform setting (as usually done in free convection) instead of a horizontally structured system as proposed earlier by, e.g. Marshall and Schott (1999), where surface cooling is confined within a specified region (usually a disc). This setting allows the analysis of interacting

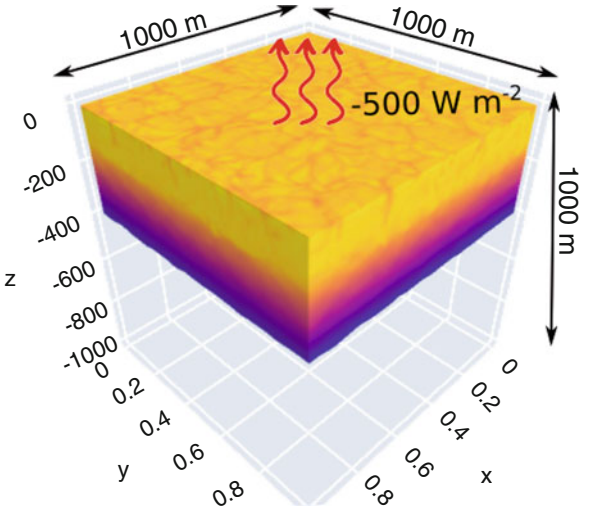

Fig. 1 Illustration of the 3D structure of the simulation after three days of simulation in a non-hydrostatic setting. The color shading is temperature

convective plumes with non-convective environment. However, such configurations are usually conducted at coarser resolution and oriented toward process studies of the geostrophic organization of convective plumes. Here, our focus is on parameterization and we wish to start with simplified settings in order to capture the essence of deep convection dynamics; interactions with a prescribed background, non-convective environment is left for further work.

From this horizontally uniform and vertically constant stratified initial condition, the model is stepped forward in time on a $100\times100\times100$ discretized grid points with isotropic resolution of 10 meters, and exposed to a constant (in time and space) cooling rate of $Q_T = -500$ W m^{-2} heat flux (Fig. 1). This leads to a cooling of upper ocean layers, which ultimately become unstable through static instabilities as a result of a negative buoyancy frequency ($N^2 = -\frac{g}{\rho}\partial_z b) < 0$, thus undergoing convection. The current settings are run with no Coriolis forcing, i.e. $f = 0$ s^{-1}; inclusion of Coriolis effects will be the subject of further work. The model is initialized with stochastic perturbations on ocean upper layers temperature decaying with depth (following Souza et al. 2020) to trigger the formation of convective plumes

$$T(x, y, z)|_{t=0} = T(z) + \sum_{(m,n)=0}^{10} \left(e^{2\pi(\mathbf{k}\cdot\mathbf{x}+\phi_{n,m})}\right) \mathcal{N}(0, 1) * \sqrt{\sigma^2} * e^{40z/Nz} \qquad (20)$$

with $T(z) = T|_{z=0} - \alpha z$, $T|_{z=0} = 3\ K$ and α is a constant defined as $\alpha = \frac{1.9e^{-6}}{g*(\alpha_T/\rho_0)}$ ($\alpha_T = 0.2048\ K^{-1}$ is the thermal coefficient, $g = 9.81\ m\ s^{-2}$ is gravity and $\rho_0 = 1024\ kg\ m^{-3}$ is reference density). The second term on the RHS of (20) is the stochastic perturbation defined as the sum of plane waves with random phase $\phi_{m,n}$

Table 1 Summary of the experiments and their numerical details. NBQ stands for the non-hydrostatic, non-Boussinesq CROCO kernel of Auclair et al. (2018); NH, Hydro and Q-NH stand for Non-Hydrostatic, Hydrostatic and Quasi-Nonhydrostatic; WENO5 and C4 for the 5-th order and the 4th-order centred advection schemes; KPP for the K-Profil Parameterization of Large et al. (1994)

Name	Kernel	Hz adv	Vert. adv	Closure	$(\Delta x, \Delta z)$	Δt	ν_w
NH	NBQ	WENO5	WENO5	–	(10, 10 m)	2.5 s	(implicit)
Hydro	Hydro	WENO5	C4	KPP	(10, 10 m)	2.5 s	–
Q-NH	Hydro	WENO5	C4	KPP	(10, 10 m)	2.5 s	1 $m^2 s^{-1}$

and of amplitude $\mathcal{N} * \sqrt{\sigma^2}$, where $\mathcal{N}$ is a Gaussian white noise distribution and $\sigma^2 = 10^{-8}\ K^2$ represents the variance of the stochastic perturbations. The random phases are drawn from an uniform distribution over the range [0, 1].

This configuration has been integrated forward in time to produce several numerical experiments in order to assess the performance of our implementation. It includes a pure Non-Hydrostatic (NH), which make use of the non-hydrostatic non-Boussinesq capabilities of CROCO (NBQ, Auclair et al. 2018), and a pure hydrostatic (Hydro) reference experiments. We then compare the solution produced by our Quasi-Nonhydrostatic (Q-NH) experiment, which includes the stochastic pressure correction, with the solutions produced by Hydro and NH.

For both Q-NH and Hydro, the KPP (Large et al. 1994) closure scheme is used to represent vertical sub-grid scale mixing. As stated in introduction, this scheme mimics vertical fluxes through a dissipative down-gradient operator. In the case of static instability associated with convective events, the dissipation coefficient is set to $K_\theta = 0.1\ m^2 s^{-1}$ in CROCO. Sensitivity tests (not shown) using TKE (Gaspar et al. 1990) closure scheme instead revealed that the choice of the closure scheme has little effect on the solution produced by our Hydro experiment.

Horizontal dissipation of vertical velocity in Q-NH is set to $\nu_w = 1\ m^2 s^{-1}$, which corresponds to high values of dissipation estimated through a Smagorinsky-like approach $\nu_{Smago} = \frac{\alpha}{2} \Delta_{xy}^2 \left((\partial_x w)^2 + (\partial_y w)^2 \right)$, with $\Delta_{xy} = 10\ m$ the horizontal resolution of our configuration, and $\alpha = 0.2$. Table 1 summarizes the different experiments, along with some numerical details.

Finally, note that all three experiments are conducted at the same isotropic resolution of 10m. Evaluating the performance of our Q-NH model for climate scale regimes (i.e. with horizontal resolution much coarser than vertical resolution) will be the subject of further work.

4 Results

We show on Fig. 2 snapshots of the vertical velocities as simulated by NH, Hydro and Q-NH after 3 days of simulation. Obviously, the NH experiment produces weaker and larger scale structures as compared to the two other experiments. It

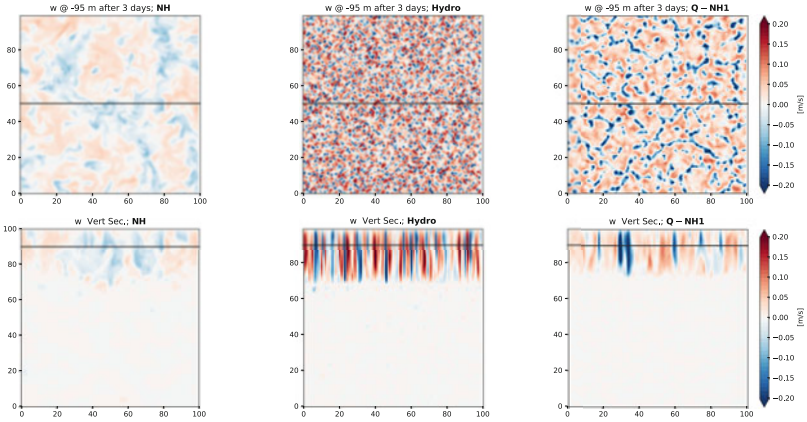

Fig. 2 Horizontal (top) and vertical (bottom) sections of vertical velocities for the Non-Hydrostatic (**NH**, left), the Hydrostatic (**Hydro**, center) and the Quasi-Nonhydrostatic (**Q-NH**, right) run. Snapshots are shown after 3 days of simulation with all other components (forcing, dissipation, stratification, resolution) held constant

is noticeable, however, that the amplitude of w in Q-NH is reduced as compared to Hydro, with larger scale structures of the convective plumes. In the Hydro experiment, plumes are localized near the grid scale and exhibit almost an order of magnitude larger vertical velocities as compared to the NH reference. The reduced vertical velocities in Q-NH and broadening of the associate spatial scale of the plumes can be interpreted as a result of the entrainment/detrainment mechanism, which is here simply represented as a purely horizontal viscous stress on vertical velocities.

Aside from vertical velocities, it is also instructive to analyse the consequence for the temperature profile, an indication of the capability of convection in producing deep water masses. Figure 3 shows the horizontally averaged temperature vertical profile, along with the rate of the Mixed Layer Depth (MLD) deepening, for the different experiments. A first remarkable result is the similarity between the temperature profiles produced by all the experiments within the MLD (i.e. $z < -300\,\mathrm{m}$). Additional tests (not shown) indeed reveal the very weak sensitivity to numerical implementation (i.e. non-hydrosatic, hydrostatic with different vertical mixing schemes), as well as the level of dissipation. The most noticeable differences between the experiments appear at the base of the mixed layer. In particular, the consequences of too strong vertical velocities in Hydro is to produce too deep water masses with a too strong penetrative convection (i.e. the envelop at the base of the mixed layer where water masses are warmer than their initial state). Although vertical velocities in Q-NH remain significantly larger than those produced by NH, the effects of horizontal viscous forces on the vertical velocities is to significantly damp the penetration of convective plumes bellow the mixed layer, inducing a strong reduction of water masses formation. The reduction of penetrative convection induces significant biases in the deepening rate of the MLD (Fig. 3, right panel).

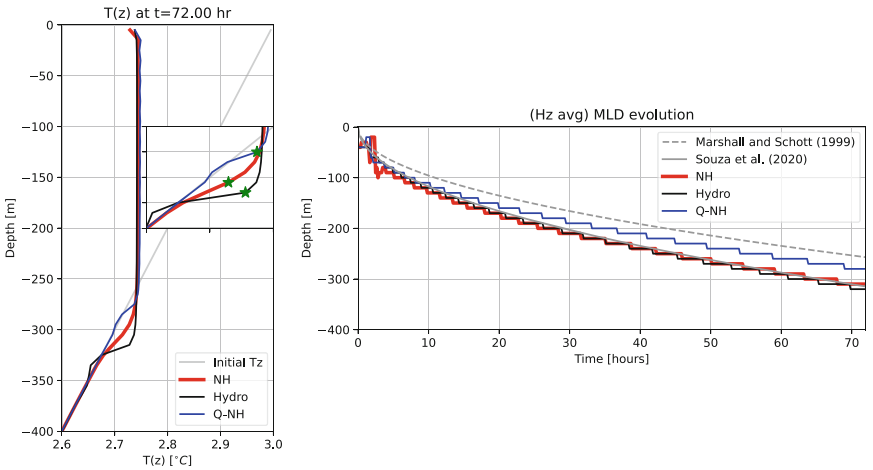

Fig. 3 Horizontally averaged temperature profiles (left) and deepening rate of the mixed layer depth (MLD, right) for the different runs at the end of the 3-day long simulations. Deepening MLD rate are compared to the analytical estimates of Marshall and Schott (1999) and Souza et al. (2020)

In Q-NH, MLD seats between the theoretical predictions of Marshall and Schott (1999) and that of Souza et al. (2020), where the former do not consider penetrative convection in their scaling while the latter do. That MLD is too shallow in Q-NH, as compared to NH, is likely a consequence of too strong dissipation imposed to the system. We note, however, that we have only considered the dissipative, rectification contribution (i.e. smooth-in-time) of the stochastic transport as a result of the strict separation assumption between martingale and smooth-in-time components. Further work are required to evaluate how the Brownian part of the stochastic transport impact the deepening of the MLD.

5 Conclusion and Perspectives

In this study, we detailed the first steps toward a full stochastic parameterization of deep ocean convection along with their implementation in the general circulation model CROCO. Our preliminary results, which consist of an approximation of the horizontal noise structure as homogeneous and isotropic, led us to recover part of the derivation provided by Klingbeil and Burchard (2013) in a deterministic case. Our results are encouraging, and we are now in a position of extending the current analysis to a fully consistent stochastic framework.

The first step in this direction will be to implement the stochastic pressure noise contribution which comes in pair with the idealized Laplacian horizontal viscosity action on vertical velocities in the context of an hydrostatic simulation of deep ocean convection (i.e. Eq. (9)). Following previous work of Pierre Dérian and

Etienne Mémin (*'Hyper-viscosity' noise for transport under location uncertainty*), we will consider a simplified expression of the stochastic transport of vertical velocity to construct our stochastic pressure noise. This approach is meant to obtain the stochastic transport associated with Laplacian or hyper-viscosity dissipation as usually implemented in OGCM. With these considerations, it is possible to express the stochastic transport of (9) as:

$$\boldsymbol{\sigma} \mathrm{d}\boldsymbol{B}_t \cdot \boldsymbol{\nabla} w = \sum_k \gamma_k \lambda_k e_k(\mathbf{x}) \tag{21}$$

with e_k a basis, defined here as Daubechies wavelets, γ_k denotes independent normally distributed variables, and λ_k are the wavelet coefficients defined as:

$$\lambda_k = \left\langle \sqrt{2\epsilon dt} |\nu^{1/2} \boldsymbol{\nabla} w|; e_k \right\rangle_{\mathcal{L}^2}, \tag{22}$$

with ϵ a scaling factor controlling the ratio of variance created by the noise to energy dissipation. Accounting for the stochastic pressure would also require considerations for the Brownian components of the stochastic transport in the horizontal momentum advection. These steps are part of further works to achieve a full, consistent implementation of LU transport in CROCO.

Acknowledgments This work is supported by the ERC project 856408-STUOD.

References

Auclair F, Bordois L, Dossmann Y, Duhaut T, Paci A, Ulses C, Nguyen C (2018) A non-hydrostatic non-Boussinesq algorithm for free-surface ocean modelling. Ocean Model 132:12–29

Bauer W, Chandramouli P, Chapron B, Li L, Mémin E (2020) Deciphering the role of small-scale inhomogeneity on geophysical flow structuration: a stochastic approach. J Phys Oceanogr 50(4):983–1003

Berkooz G, Holmes P, Lumley JL (1993) The proper orthogonal decomposition in the analysis of turbulent flows. Annual review of fluid mechanics 25(1):539–575

Debreu L, Marchesiello P, Penven P, Cambon G (2012) Two-way nesting in split-explicit ocean models: Algorithms, implementation and validation. Ocean Model 49:1–21

Delorme BL, Thomas LN, Marchesiello P, Gula J, Roullet G, Molemaker MJ (2021) Enhanced abyssal mixing in the equatorial pacific associated with non-traditional effects. J Phys Oceanogr 51(6):1895–1914

Gaspar P, Grégoris Y, Lefevre JM (1990) A simple eddy kinetic energy model for simulations of the oceanic vertical mixing: Tests at station papa and long-term upper ocean study site. Journal of Geophysical Research: Oceans 95(C9):16,179–16,193

Gill AE (1982) Atmosphere-ocean dynamics, vol 30. Academic press

Giordani H, Bourdallé-Badie R, Madec G (2020) An eddy-diffusivity mass-flux parameterization for modeling oceanic convection. Journal of Advances in Modeling Earth Systems 12(9):e2020MS002,078

Heuzé C (2017) North atlantic deep water formation and amoc in cmip5 models. Ocean Sci 13(4):609–622

Heuzé C (2021) Antarctic bottom water and north atlantic deep water in cmip6 models. Ocean Sci 17(1):59–90

Hourdin F, Musat I, Bony S, Braconnot P, Codron F, Dufresne JL, Fairhead L, Filiberti MA, Friedlingstein P, Grandpeix JY, et al (2006) The lmdz4 general circulation model: climate performance and sensitivity to parametrized physics with emphasis on tropical convection. Clim Dyn 27:787–813

Klingbeil K, Burchard H (2013) Implementation of a direct nonhydrostatic pressure gradient discretisation into a layered ocean model. Ocean Model 65:64–77

Large WG, McWilliams JC, Doney SC (1994) Oceanic vertical mixing: A review and a model with a nonlocal boundary layer parameterization. Rev Geophys 32(4):363–403

Marshall J, Schott F (1999) Open-ocean convection: Observations, theory, and models. Reviews of Geophysics 37(1):1–64

Marshall J, Hill C, Perelman L, Adcroft A (1997) Hydrostatic, quasi-hydrostatic, and nonhydrostatic ocean modeling. Journal of Geophysical Research: Oceans 102(C3):5733–5752

Masson-Delmotte V, Zhai P, Pirani A, Connors SL, Péan C, Berger S, Caud N, Chen Y, Goldfarb L, Gomis M, et al (2021) Climate change 2021: the physical science basis. Contribution of working group I to the sixth assessment report of the intergovernmental panel on climate change 2

Mémin E (2014) Fluid flow dynamics under location uncertainty. Geophys Astrophys Fluid Dynamics 108(2):119–146

Resseguier V, Mémin E, Chapron B (2017) Geophysical flows under location uncertainty, part i random transport and general models. Geophysical & Astrophysical Fluid Dynamics 111(3):149–176

Shchepetkin AF, McWilliams JC (2005) The regional oceanic modeling system (ROMS): a split-explicit, free-surface, topography-following-coordinate oceanic model. Ocean modelling 9(4):347–404

Souza AN, Wagner G, Ramadhan A, Allen B, Churavy V, Schloss J, Campin J, Hill C, Edelman A, Marshall J, et al (2020) Uncertainty Quantification of Ocean Parameterizations: Application to the K-Profile-Parameterization for Penetrative Convection. Journal of Advances in Modeling Earth Systems 12(12):e2020MS002,108

Suselj K, Kurowski MJ, Teixeira J (2019) A unified eddy-diffusivity/mass-flux approach for modeling atmospheric convection. J Atmos Sci 76(8):2505–2537

Tucciarone FL, Mémin E, Li L (2023) Primitive equations under location uncertainty: Analytical description and model development. In: Stochastic Transport in Upper Ocean Dynamics Annual Workshop, Springer, pp 287–300

Umlauf L, Burchard H (2003) A generic length-scale equation for geophysical turbulence models. J Mar Res 61(2):235–265

Zhang R, Sutton R, Danabasoglu G, Kwon YO, Marsh R, Yeager SG, Amrhein DE, Little CM (2019) A review of the role of the Atlantic meridional overturning circulation in Atlantic multidecadal variability and associated climate impacts. Rev Geophys 57(2):316–375